N7 and C8 coordinated purine complexes of $[(NH_3)_5Os^{III}]$. Crystal structures of 7-$[9MeHyp(NH_3)_5Os]Cl_3 \cdot H_2O$ and 8-$[1,3,7Me_3Xan(NH_3)_5Os]Cl_3 \cdot 2H_2O$

Arden Johnson, Lynne A. O'Connell and M.J. Clarke*
The Merkert Chemistry Center, Boston College, Chestnut Hill, MA 02167 (USA)

(Received January 26, 1993; revised April 13, 1993)

Abstract

Pentaammineosmium(III) coordinates to both the N7 and C8 positions of purine rings. The compound 7-$[9MeHyp(NH_3)_5Os]Cl_3 \cdot H_2O$ crystallizes in the orthorhombic space group *Pnma* (No. 62) with the unit cell parameters: $a = 11.542(2)$, $b = 6.9841(8)$, $c = 21.960(3)$ Å and $Z = 4$. The compound 8-$[1,3,7Me_3Xan(NH_3)_5Os]Cl_3 \cdot 2H_2O$ crystallizes in the monoclinic space group $P2_1/c$ (No. 14) with the unit cell parameters: $a = 7.1228($ Å, $b = 14.613(1)$, $c = 19.667(1)$ Å, $\beta = 91.782(9)°$ and $Z = 4$. The Os–C bond in the latter structure is 2.039(9) Å and the imidazolylidine ligand exerts a slight *trans* influence seen in the lengthening of the Os–N_{ax} distance (2.172(8) Å) by about 0.05 Å relative to the average of the equatorial Os–N_{eq} value of 2.123(8) Å. The spectroscopic, electrochemical and structural properties of these and additional N-bound purine complexes are compared with those of similar N7 and C8 ruthenium(III) species.

Introduction

Platinum group metal complexes with ammine ligands often exhibit antitumor activity by binding to purine nitrogen sites on DNA [1–3]. Both platinum and ruthenium complexes of nucleoside ligands have exhibited interesting linkage isomerization reactions [4–9]. While these usually involve metal ion movement between adjacent atoms, in one instance Pt^{II} moves to a site several Ångstroms away [4]. Recently developed chemistry of $[(NH_3)_5Os^{II}]$ [9–12] has led to the synthesis of series of complexes in which the Os^{II} adds across double bonds even in aqueous solution [13]. Moreover, this moiety reacts with the olefinic site of pyrimidine ligands [12]. The preference of $[(NH_3)_5Os^{III}]$ for nitrogen sites and $[(NH_3)_5Os^{II}]$ for olefinic sites suggests that interesting, redox-induced long-range metal migrations of these ions might occur around the perimeter of purine ligands or between such sites in nucleic acids. Herein we report on the synthesis and characterization of a series of complexes of the general type $[L(NH_3)_5Os^{III}]$, where L = 1-methylguanosine, 9-methylhypoxanthine, theophylline and caffeine, in which the metal ion coordinates to one of the ring imines or, in the case of caffeine, to C8.

*Author to whom correspondence should be addressed.

Experimental**

The starting material, $[N_2(NH_3)_5Os]Cl_2$, was made by the reaction of $N_2H_4 \cdot H_2O$ on the commercially available $(NH_4)_2[Cl_6Os]$ [14, 15]. $[(NH_3)_5Os(CF_3SO_3)](CF_3SO_3)_2$ was prepared by the bromine oxidation of $[N_2(NH_3)_5Os]Cl_2$ in neat triflic acid [16]. Purine complexes were prepared by dissolving 50 mg of the ligand in 10 ml propylene carbonate and adding 50 mg of $[Os(NH_3)_5CF_3SO_3](CF_3SO_3)_2$ [17]. The mixture was stirred at 50–60 °C until a color change became apparent (1–22 h). The reaction mixture was cooled, filtered to remove undissolved ligand, and diluted with 10 ml acetone before gradually adding diethyl ether with vigorous shaking to precipitate a flocculent material. This was filtered off and the residue redissolved in a small amount of acetone. After this solution was filtered, diethyl ether was added to reprecipitate the solid product, which was filtered, washed with ether and dried under suction. Typical yields are ~30 mg of amorphous powder or microcrystals, ranging in color from yellow to orange.

**Abbreviations: 9MeHyp, 9-methylhypoxanthine; 9MeXan, 9-methylxanthine; $1,3Me_2Xan$, 1,3-dimethylxanthine (theophylline); $1,7Me_2Xan$, 1,7-dimethylxanthine; $1,3,7Me_3Xan$, 1,3,7-trimethylxanthine (caffeine); Gua, guanine; Guo, guanosine; 1MeGuo, 1-methylguanosine.

0020-1693/93/$6.00

Preparation of 7-[9MeHyp$(NH_3)_5Os$]$Cl_3 \cdot H_2O$

A solution containing 50 mg 9MeHyp and 50 mg $[Os(NH_3)_5CF_3SO_3](CF_3SO_3)_2$ in 10 ml propylene carbonate was stirred at 50–60 °C for 4 h to yield a yellow solution. The mixture was cooled to room temperature, diluted to ~100 ml with distilled water and loaded onto a SP-Sephadex-C25 column. The column was extensively eluted with water to remove unreacted ligand, before carefully adding 0.1 M HCl and increasing the concentration so that a yellow band was eluted with 0.3 M HCl. This fraction was rotary-evaporated to dryness, the residue dissolved in a minimum of 0.25 M HCl, and yellow, crystalline material was obtained upon vapor diffusion of ethanol. *Anal.* Calc. for $H_{23}C_6N_9O_2OsCl_3$: H, 4.22; C, 13.11; N, 22.93. Found: H, 4.03; C, 12.96; N, 22.45%. IR (cm^{-1}): ν(N–H) = 3216; ν(C=O) = 1717. ^1H NMR (δ ppm): pH 2.4, H2, 6.5; H8, −20.5; CH_3, 9.9; pH 12.0, H2, 7.4, H8, −21.9; CH_3, 12.6.

7-[9MeXan$(NH_3)_5Os$]$Cl_3 \cdot 0.5H_2O$

This compound was prepared as above but with heating for 22 h. The yellow band eluted with 0.35 M HCl. *Anal.* Calc. for $H_{21}C_6N_9O_2OsCl_3 \cdot 0.5H_2O$: H, 3.98; C, 12.94; N, 22.64. Found: H, 3.63; C, 13.62; N, 21.31%. IR (cm^{-1}): ν(N–H) = 3258; ν(C=O) = 1693, 1728. UV–Vis (λ (nm), ϵ(10^3 M^{-1} cm^{-1})): 243, 12.5; 280, 8.2; 342, 1.3; 466, 0.8. ^1H NMR (δ ppm): pH 0.7, H8, −23.9; CH_3, 9.0.

7-[1,3Me_2Xan$(NH_3)_5Os$]$Cl_3 \cdot 3H_2O$

This compound was prepared as above but with heating for 3 h to yield an orange solution. The desired yellow band eluted with 0.3 M HCl. *Anal.* Calc. for $H_{29}C_7N_9O_5OsCl_3$: H, 4.75; C, 13.65; N, 20.47. Found: H, 4.67; C, 13.22; N, 20.33%. IR (cm^{-1}): ν(N–H) = 3234; ν(C=O) = 1713, 1678. UV–Vis, pH 1, 0.1 M CF_3SO_3H, (λ (nm), ϵ(10^3 M^{-1} cm^{-1})): 231, 10.4; 265, 8.0; 350, 0.24; 420, 0.10. ^1H NMR (δ ppm): pH 0.63, H8, −24.2; CH_3(1), 3.47; CH_3(3), 2.94.

7-[1MeGuo$(NH_3)_5Os$]$Cl_3 \cdot 4H_2O$

This compound was prepared as above but with heating for 2 h to yield an orange–yellow solution. A small orange band was eluted with 0.2 M HCl and was followed by the desired orange–yellow band, which eluted with 0.3 M HCl. An orange solid was obtained by vapor diffusion. *Anal.* Calc. for $H_{38}C_{11}N_{10}O_9OsCl_3$: H, 5.10; C, 17.59; N, 18.65. Found: H, 4.95; C, 16.19; N, 18.55%. IR (cm^{-1}): ν(N–H) = 3227; ν(C=O) = 1675. UV–Vis, pH 1, 0.1 M CF_3SO_3H, (λ (nm), ϵ(10^3 M^{-1} cm^{-1})): 257, 12.4; 270, 6.9; 354(sh), 0.27; 446, 0.18. ^1H NMR (δ ppm): pH 6, H8, −24.4; CH_3(1), 3.4; H1′, 10.0; H2′–H5′, 3.6–4.68.

9-[1,7Me_2Xan$(NH_3)_5Os$]$Cl_3 \cdot 3H_2O$

This compound was prepared as above but with heating for 1.5 h. A bright yellow band eluted with 0.25 M HCl. *Anal.* Calc. for $H_{24}C_7N_9O_2OsCl_3 \cdot 3H_2O$: H, 4.75; C, 13.65; N, 20.47. Found: H, 4.10; C, 13.51; N, 19.95%. UV–Vis, pH 1., 0.1 M CF_3SO_3H (λ (nm), ϵ(10^3 M^{-1} cm^{-1})): 231, 10.4; 265, 8.0; 350, 0.24; 420, 0.10. ^1H NMR (δ ppm): pH 2–8, CH_3(1), 10.1; CH_3(7), 14.4.

8-[1,3,7Me_3Xan$(NH_3)_5Os$]$Cl_3 \cdot 2H_2O$

A solution containing 50 mg 1,3,7Me_3Xan and 50 mg $[Os(NH_3)_5CF_3SO_3](CF_3SO_3)_2$ in 10 ml methanol was sparged with argon for 45 min. Zn amalgam was added and the reaction was allowed to proceed for 60 min with continuous Ar bubbling. The amalgam was removed from the yellow solution, which was then oxidized with O_2 for 10 min. The orange solution was diluted with distilled water and chromatographed in the same manner as above. An orange band eluted with 0.3 M HCl and an orange solid was obtained by vapor diffusion of ethanol. *Anal.* Calc. for $H_{29}C_8N_9O_4OsCl_3$: H, 4.78; C, 15.70; N, 20.60. Found: H, 4.77; C, 15.34; N, 20.66%. IR (cm^{-1}): ν(N–H) = 3213; ν(C=O) = 1680, 1697. UV–Vis (λ (nm), ϵ (10^3 M^{-1} cm^{-1})): pH 1, 0.1 M CF_3SO_3H, 248, 7.6; 291, 8.9; 356, 0.68; 374(sh), 0.4; 472, 0.54. pH 10, 0.1 M CF_3SO_3Li, 298, 9.4; 362, 0.97; 388, 0.4; 506, 0.54.

Compound characterization

Elemental analyses were performed by Robertson Laboratories. UV–Vis spectra were obtained on a Cary model 2400. IR spectra were determined on KBr pellets in a Nicolet model 510 FT-IR spectrophotometer. ^1H NMR spectra were performed on samples in D_2O solution on a Varian 300 XL Fourier transform spectrometer. Electrochemical measurements were performed by cyclic or square-wave voltammetry in 0.1 M $LiCF_3SO_3$ on a versatile electrochemical apparatus constructed in this laboratory [7]. A carbon paste or platinum button working electrode, Ag/AgCl reference electrode and platinum wire auxiliary electrode were used in all measurements. Reduction potentials were determined as the peak potential in square-wave voltammetric scans and by the average of the anodic and cathodic peak potentials from cyclic voltammetric scans. All potentials were internally referenced against the $[(NH_3)_6Ru]^{3+,2+}$ couple (57 mV versus NHE).

Crystal structure determination

Pertinent crystal data for both 7-[9MeHyp$(NH_3)_5Os$]-$Cl_3 \cdot H_2O$ and 8-[1,3,7Me_3Hyp$(NH_3)_5Os$]$Cl_3 \cdot 2H_2O$ are given in Table 1 and crystallographic coordinates for the non-hydrogen atoms in both structures are listed in Table 2. Single crystals of 7-[9MeHyp$(NH_3)_5Os$]-

TABLE 1. Crystallographic data for 7-[9MeHyp$(NH_3)_5Os]Cl_3 \cdot H_2O$ and 8-[1,3,7Me_3Xan$(NH_3)_5Os]Cl_3 \cdot 2H_2O$[a]

Formula	$C_6H_{23}N_9O_2Cl_3Os$	$C_8H_{29}N_9O_4Cl_3Os$
Formula weight	549.88	611.9
Space group, crystal system	*Pnma* (No. 62), orthorhombic	$P2_1/c$ (No. 14), monoclinic
Cell constants		
a (Å)	11.542(2)	7.1228(9)
b (Å)	6.9481(8)	14.613(1)
c (Å)	21.960(6)	19.667(1)
β (°)		91.782(9)
Cell volume (Å^3)	1761(1)	2046.1(2)
Z (FW/unit cell)	4	4
T (°C)	22(1)	23(1)
Radiation source (graphite monochromated), λ (Å)	Mo Kα, 0.71069	Cu Kα, 1.54178
D_{calc} (g/cm^3)	2.074	1.987
μ (cm^{-1})	77.24	157.73
Relative transmission factors	0.52–1.0	0.83–1.0
Total no. reflections collected	2364	3129
Observed reflections[b]	1793	2689
$R = \frac{\Sigma(\lvert F_o\rvert - \lvert F_c\rvert)}{\Sigma\lvert F_o\rvert}$	0.034	0.040
$R_w = \left[\frac{\Sigma w(\lvert F_o\rvert - \lvert F_c\rvert)^2}{\Sigma w\lvert F_o\rvert^2}\right]^{1/2}$[c]	0.050	0.055

[a]All calculations were performed by using the TEXSAN-TEXRAY Structure Analysis Package, Molecular Structure Corp., 1985. [b]Reflections with $I > 3\sigma(I)$ were retained as observed and used in the solution and refinement of the structure. Three standard reflections were monitored with a limit of 0.2% variation. Function minimized $\Sigma w(\lvert F_o\rvert - \lvert F_c\rvert)^2$. [c]Weighting scheme: $w = 4F_o^2/\sigma^2(F_o)^2$.

$Cl_3 \cdot H_2O$ were grown by slow solvent diffusion of ethanol into an aqueous solution of the compound. A suitable crystal was mounted on a glass fiber, which was placed in the beam of a Rigaku AFC5R diffractometer. Space group assignment was based on the systematic absences of $0kl$: $k+l \neq 2n$ and $hk0$: $h \neq 2n$. Intensities of three representative reflections, which were measured after every 150 reflections, remained constant throughout data collection so that no decay correction was necessary; however, an empirical absorption correction was applied. The Os atom was located by direct methods and the structure solved from difference Fourier maps [18, 19]. The non-hydrogen atoms were refined anisotropically. Hydrogen atoms on the purine ring were located from difference maps. The ammine protons were included in the structure factor calculation in idealized positions (C–H = 0.95, N–H = 0.87, O–H = 0.82 Å) [20]. All hydrogens were assigned isotropic thermal parameters, which were 20% greater than the B_{eq} value of the atom to which they were bonded. Refinement was by full-matrix least-squares. Neutral atom scattering factors [21] and anomalous dispersion effects were included in F_{calc} [22]; the values for $\Delta f'$ and $\Delta f''$ were those of Cromer and Weber [21].

Solution of the structure of 8-[1,3,7Me_3Hyp$(NH_3)_5Os]$-$Cl_3 \cdot 2H_2O$ was similarly performed, except that Cu Kα radiation was used. Based on systematic absences of $h0l$: $l \neq 2n$ and $0k0$: $k \neq 2n$ and the successful solution and refinement of the structure, the space group was determined to be $P2_1/c$ (No. 14). An absorption correction was applied. Hydrogen atoms on ammines and methyls were placed in calculated positions. Hydrogens H26, H27 and H28 on the water molecules were located from difference maps.

Results

Structures

Figure 1 illustrates the structure of [9MeHyp-$(NH_3)_5Os]^{3+}$ in which the essentially octahedral Os is coordinated to the N7 of the purine ring. The metal atom and the 9MeHyp ligand lie on a crystallographic mirror plane located at $y = \frac{1}{4}$ and so are crystallographically required to be in the same plane. The chlorides and the water of hydration also lie on the same mirror plane. The bond distances are summarized in Table 3, and all the Os–N bond lengths are typical of Os–N single bonds [23]. O6 is internally hydrogen bonded to the *cis*-ammine ligands (O6–N11 = 2.909(9) Å) as well as to N10 on a symmetry related molecule (O6–N10 = 2.73(1) Å). The water of hydration is situated near O6 (O1–O6 = 3.537(3) Å) and is hydrogen bonded to an ionic chloride (O1–Cl3 = 3.14(1) Å). There is some stacking between the N3–C2 region of symmetry related hypoxanthine rings at a distance of 3.539(3) Å.

Figure 2 shows the structure of [1,3,7Me_3Xan-$(NH_3)_5Os]^{3+}$ in which the coordination sphere around

TABLE 2. Crystallographic coordinates for atoms in 7-[9MeHyp$(NH_3)_5Os]Cl_3 \cdot H_2O$ and 8-[1,3,7Me_3Xan$(NH_3)_5Os]Cl_3 \cdot 2H_2O$

Atom	x	y	z	B_{eq}
7-[9MeHyp$(NH_3)_5Os]Cl_3 \cdot H_2O$				
Os	0.6281	0.2500	0.6462	2.3
Cl(1)	0.3704	0.2500	0.4963	3.6
Cl(2)	0.2585	0.2500	0.6718	3.7
Cl(3)	1.0027	0.2500	0.2288	4.1
O(1)	0.6056	0.2500	0.1385	4.9
O(6)	0.4328	0.2500	−0.1614	4.3
N(1)	1.0507	0.2500	0.5777	2.7
N(3)	0.4883	0.2500	0.0232	3.1
N(7)	0.2333	0.2500	−0.0678	2.4
N(9)	0.2799	0.2500	0.0304	2.4
N(10)	0.5216	0.2500	0.7232	3.2
N(11)	0.7248	0.0313	0.6900	3.1
N(12)	0.5209	0.0349	0.6079	3.0
C(2)	1.0696	0.2500	0.5186	3.2
C(4)	0.3797	0.2500	−0.0021	2.4
C(5)	0.3504	0.2500	−0.0630	2.3
C(6)	0.4422	0.2500	−0.1055	2.8
C(8)	0.1936	0.2500	−0.0115	2.6
C(9)	0.2656	0.2500	0.0967	2.9
8-[1,3,7Me_3Xan$(NH_3)_5Os]Cl_3 \cdot 2H_2O$				
Os	0.7850	0.0833	0.3271	1.0
Cl(1)	0.3047	0.0686	0.4550	2.6
Cl(2)	0.2396	0.1357	0.2068	3.4
Cl(3)	0.6832	0.3543	0.2559	2.2
O(1)	0.1166	0.1866	0.6285	4.7
O(2)	0.6457	0.2140	−0.0476	2.9
O(5)	0.1027	0.2481	0.9857	6.2
O(6)	0.7837	−0.0715	0.0329	3.4
N(1)	0.7202	0.0721	−0.0070	2.0
N(3)	0.6700	0.1976	0.0667	1.9
N(7)	0.7737	0.0136	0.1772	1.3
N(9)	0.7177	0.1596	0.1870	1.4
N(10)	0.8215	0.0938	0.4367	2.2
N(11)	0.9605	0.2007	0.3221	1.9
N(12)	0.5431	0.1663	0.3316	1.9
N(13)	0.6106	−0.0328	0.3443	2.1
N(14)	1.0327	0.0023	0.3273	2.4
C(2)	0.6782	0.1651	0.0006	2.0
C(4)	0.7120	0.1396	0.1197	1.5
C(5)	0.7467	0.0505	0.1114	1.5
C(6)	0.7531	0.0097	0.0459	1.8
C(8)	0.7551	0.0821	0.2237	1.4
C(9)	0.6188	0.2921	0.0789	3.0
C(10)	0.7277	0.0390	−0.0769	2.9
C(11)	0.8087	−0.0812	0.1919	2.4

the Os is also essentially octahedral with the purine coordinated through C(8). Bond distances are summarized in Table 2 and indicate that the Os–C(8) interaction exerts a slight *trans* influence, which is seen in the lengthening of the Os–N_{ax} distance by about 0.05 Å relative to the average of the equatorial Os–N_{eq} value of 2.123(8) Å. The Os is displaced from the plane defined by the *cis* ammines toward C8 by 0.084 Å. The

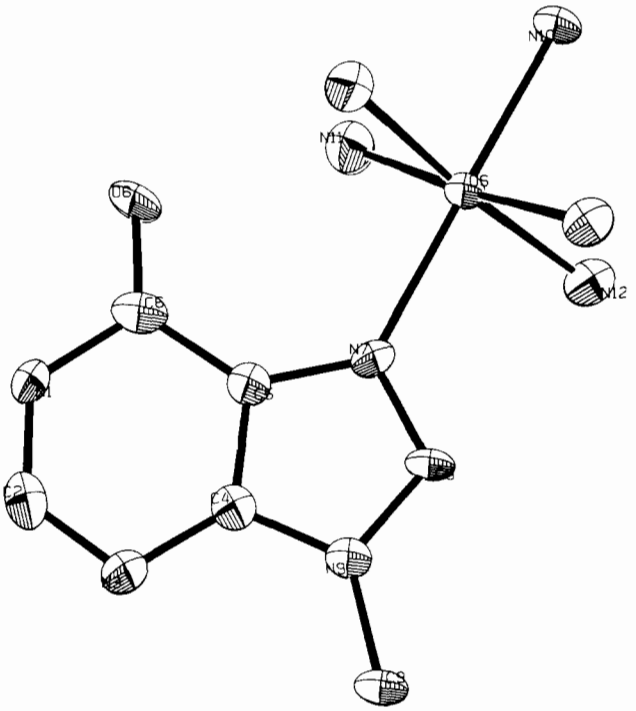

Fig. 1. ORTEP diagram of 7-[9MeHyp$(NH_3)_5Os^{III-II}$].

mean deviation in the plane of the purine is 0.015(9) Å. There is essentially no stacking of the purine rings in the packing diagram. A steric repulsion between the C11 methyl group and the *cis* ammine ligands causes the Os–C8–N7 angle (131.8(6)°) to be somewhat larger than the Os–C8–N9 angle (122.3(6)°). There is extensive hydrogen bonding evident in the crystal packing: the two waters of hydration are H-bonded (O1–O5 = 2.98(1) Å); O5 and O6 are H-bonded at 2.74(1) Å; Cl1 and O5 are separated by only 3.10(1) Å; Cl2 and O1 are at 3.130(9) Å, and Cl3 is situated between N9, N11 and N12 on the same molecule at distances of 3.166(8), 3.245(8) and 3.295(8) Å, respectively.

Spectra and electrochemistry

The orange color of this series of complexes derives from a ligand-to-metal charge transfer transition that shifts to lower energy as the purine ligand is ionized. The pK_a of the theophylline complex was determined spectrophotometrically as 2.9 ± 0.4. In this case the visible LMCT at 434 nm ($\epsilon = 250\ M^{-1}\ cm^{-1}$) shifts to 461 nm ($\epsilon = 510\ M^{-1}\ cm^{-1}$) upon loss of the N9 proton. Consistent with the spectrophotometric pK_a, a plot of reduction potential versus pH for 7-[1,3Me_2Xan-$(NH_3)_5Os^{III-II}$] is constant at −0.54 V but shows a distinct downward curvature around pH 2.9 decreasing to a constant −0.83 V above pH 5; however, two couples were evident around pH 4 and the slope (~234 mV/pH) in the pH-dependent region is four times steeper than the 58.5 mV/pH expected for a 1H/1e process, when fit to the equation:

TABLE 3. Bond lengths (Å) in 7-[9MeHyp$(NH_3)_5Os]^{3+}$ and 8-[1,3,7Me_3Xan$(NH_3)_5Os]^{3+}$

	7-[9MeHyp$(NH_3)_5Os]Cl_3 \cdot H_2O$	8-[1,3,7Me_3Xan$(NH_3)_5Os]Cl_3 \cdot 2H_2O$
Os–C8		2.039(9)
Os–N7	2.107(8)	
Os–N10	2.089(8)	2.172(8)
Os–N11	2.117(6)	2.129(8)
Os–N12	2.115(6)	2.112(7)
Os–N13		2.127(8)
Os–N14		2.125(8)
O2–C2		1.21(1)
O6–C6	1.23(1)	1.23(1)
N1–C2	1.32(1)	1.40(1)
N1–C6	1.39(1)	1.40(1)
N1–C10		1.46(1)
N3–C2	1.31(1)	1.39(1)
N3–C4	1.37(1)	1.37(1)
N3–C9		1.45(1)
N7–C5	1.36(1)	1.41(1)
N7–C8	1.32(1)	1.36(1)
N7–C11		1.43(1)
N9–C4	1.36(1)	1.36(1)
N9–C8	1.36(1)	1.36(1)
N9–C9	1.47(1)	
C4–C5	1.38(1)	1.34(1)
C5–C6	1.41(1)	1.42(1)

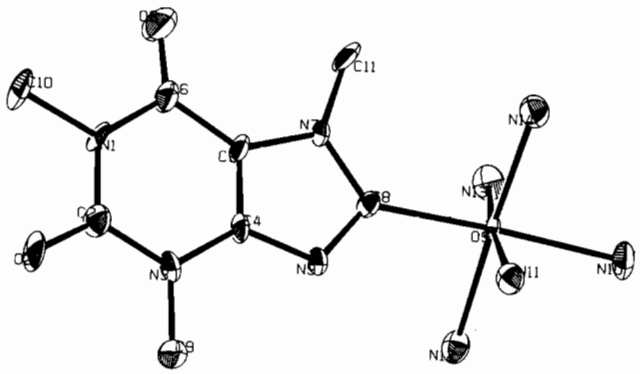

Fig. 2. ORTEP diagram of 8-[1,3,7Me_3Xan$(NH_3)_5Os^{III}$].

$$E_h = E^\circ + m \log \frac{[H^+] + K_{ox}}{[H^+] + K_{red}}$$

where E_h is the reduction potential at a given pH, m is the slope, K_{ox} is the ionization constant for the Os^{III} form of the complex, and K_{red} is the ionization constant for the reduced complex. Similar behavior is observed for [9MeHyp$(NH_3)_5Os^{III-II}$] with $E^\circ = -0.53$ at low pH and the onset of curvature at pH ~6.2 with the reduction potential again constant at −0.65 V above pH 8.

The caffeine complex, [1,3,7Me_3Xan$(NH_3)_5Os^{III}$], exhibits a spectrophotometric pK_a of approximately 5.2. The Pourbaix plot for this complex is consistent with a pK_a of 5.2 ($E^\circ = -0.18$ V at pH < 5), but also exhibits a slope at least four times that expected for a 1H/1e process. Above pH 7, the potential is again independent of pH at $E = -0.43$ V. Between pH 5.0 and 5.2, two couples are evident about 150 mV apart.

The ^1H NMR spectrum of [1,3Me_2Xan$(NH_3)_5Os^{III}$] is similar to that of the analogous Ru^{III} compound, so that assignments of the methyl resonances were made by analogy [24]. A minor difference is that the $CH_3(3)$ resonance is shifted 0.29 ppm upfield by Os^{III} and 0.7 ppm downfield by Ru^{III}. Similarly, the spectrum of [9MeHyp$(NH_3)_5Os^{III}$] is analogous to that of [9MeGua$(NH_3)_5Ru^{III}$] as is the spectrum of [1MeGuo-$(NH_3)_5Os^{III}$] similar to that of [Guo$(NH_3)_5Ru^{III}$], except that in the osmium complexes the paramagnetic shifts are less pronounced.

Discussion

Spectra

The decrease in energy and increase in intensity of the visible band (430–470 nm) upon ligand ionization or on addition of the electron donating amine group verifies that this is an LMCT transition. The origin of the bands around 350 nm is less certain, since they exhibit only minor shifts upon ligand deprotonation or addition of the amine. Nevertheless, the near UV and visible transitions in complexes of the type [L$(NH_3)_5Os^{III}$], where L is a purine ligand, bear strong similarities to those of analogous Ru^{III} complexes, which are believed to be $\pi \rightarrow d_\pi$ transitions [6, 25, 26], so that similar LMCT origins are likely. By analogy with single-crystal polarized spectra and *ab initio* calculations

on complexes of the type, $[L(NH_3)_5Ru^{III}]$, where L is an imidazole derivative, these transitions might be assigned as $\pi_1 \rightarrow d_{xz}$ for the visible band and $\pi_2 \rightarrow d_{xz}$ for the near-UV transition [27]. If so, then the lower energy of the near-UV bands and higher energy of the visible transitions suggest that the π_1 and π_2 purine orbitals interact differently with the d_π orbital in Ru^{III} and Os^{III}. Mixing of the charge transfer with spin–orbit coupling, as has been shown for other Os^{III} complexes with heterocyclic ligands, may be involved [28].

The decrease in ^1H NMR paramagnetic shifts between analogous Ru^{III} and Os^{III} complexes is also consistent with somewhat different π–d_π interactions. This could derive from less π-donation to Os^{III} resulting in a lower transfer of d_π spin density to the ligand. In further harmony with less π-bonding to Os^{III} is the slightly higher pK_a for 7-$[1,3Me_2Xan(NH_3)_5Os^{III}]^{3+}$ relative to the analogous Ru^{III} species. Owing to the structural similarities cited below, metal-induced changes in ligand acidity must arise from bonding rather than through-space electrostatic differences.

Structure

The crystal structure of 7-$[9MeHyp(NH_3)_5Os]Cl_3 \cdot H_2O$ unequivocally establishes the expected result that $(NH_3)_5Os^{III}$ will bind at the sterically free lone pair of N7 on purine ligands. Spectroscopic analogies between this compound and 7-$[1MeGuo(NH_3)_5Os]Cl_3$ indicate that both guanine and hypoxanthine nucleosides also coordinate Os^{III} through this site. The structure of 8-$[1,3,7Me_3Xan(NH_3)_5Os]Cl \cdot 2H_2O$ indicates that an ylidene structure is possible, when no other suitable sites are readily available.

The analogous bond distances and angles (including those around the metal) in 7-$[9MeHyp(NH_3)_5Os]^{3+}$ are essentially identical to those in 7-$[Hyp(NH_3)_5Ru]^{3+}$, which crystallizes in the same space group and with unit cell parameters very similar to $[Hyp(NH_3)_5Ru]Cl_3 \cdot 3H_2O$ [29]. Consequently, the steric consequences of $[L(NH_3)_5M]^{3+}$ are identical for M = Ru or Os, when L is an N-coordinated imidazole or purine ligand.

When compared with the free caffeine ligand [30], the structure of 8-$[1,3,7Me_3Xan(NH_3)_5Os]^{3+}$ is essentially identical with only a 0.03 Å lengthening of the N7–C5 bond being of possible statistical significance. When compared with a similar Ru^{III} complex, 8-$[(1,3,7Me_3Xan)Cl_2(NH_3)_3Ru]Cl \cdot H_2O$ [31], the C8–N7 bond is significantly longer in the osmium compound by 0.05 Å. A 0.03 Å contraction in the C8–N9 bond in the osmium complex (relative to the ruthenium) is also of possible significance. An important difference between these two complexes is that the *trans* labilizing ability of the ylidene carbon induces substitution by a chloride in the case of ruthenium, but not with osmium. (Because of harsher reaction conditions, a *cis* ammine in the Ru^{III} structure was also substituted by a chloride [26].) Nevertheless, a *trans* influence is evident in the present structure in the 0.05 Å lengthening of the Os–N10 bond relative to the average equatorial Os–N distance. In comparing the Ru and Os structures, changes in π-bonding between the metal and the caffeine might be modulated by the π-donor ability of the *trans* ligand and so may also have an effect on the π-bonding between C8 and the adjacent nitrogens, which are equivalent in the osmium structure but differ by 0.05 Å in the ruthenium. Also of possible significance is a shortening of the bridging C4–C5 bond (0.026 Å for Os and 0.037 Å for Ru) relative to that of free caffeine [30], which may indicate a transmission of π-effects into the pyrimidine ring.

Electrochemistry

The reduction potentials of Os^{III} complexes are generally 0.5–0.8 V more negative than the $E°$ values for the corresponding Ru^{III} complexes [28], so that the $E°$ values for the neutral ligand Os^{III} complexes reported here are in the ranges expected. Since C-bound imidazolylidenes are strong π-acceptors [26], the reduction potentials of such complexes are higher by about 0.22 V for $Ru^{III/II}$ and 0.36 V for $Os^{III/II}$ relative to similar N-bound complexes.

Of particular interest is the anomalous pH dependence exhibited by the Os^{III} reduction potentials. While the Pourbaix plots are consistent with multiple proton ionizations, this is unlikely unless some other transformation also occurs in the molecule. $[(NH_3)_5Os^{II}]$ can migrate from an η^1-binding site on heteroatoms to olefinic bonds to which it binds in an η^2-fashion [13], and has been observed to bind across C4–C5 of uracil [12]; however, these species generally show much more *positive* reduction potentials in the range 0.1–0.5 V. Consequently, if reduction-induced linkage isomerization is occurring in these complexes, it is likely to involve movement to a substantially more basic (and probably anionic) site. One possibility is that the metal migrates through π-bonded transient species to the deprotonated site. On the other hand, the presence of two electrochemical couples is also evident in the Pourbaix behavior of a complex as simple as $[(H_2O)(NH_3)_5Os^{III/II}]$ [32] and a seven-coordinate dihydrogen complex, η^2-$[H_2(NH_3)_5Os^{II}]$ [33], has recently been reported [32], which suggests that an unusual proton equilibrium might occur directly on the metal.

Acknowledgement

This work was supported by PHS Grant GM-26390.

References

1 M.J. Clarke (ed.), *Ruthenium and Other Non-Platinum Metal Complexes in Cancer Chemotherapy,* Vol. 10, Springer, Heidelberg, 1989.
2 W.I. Sundquist and S.J. Lippard, *Coord. Chem. Rev., 100* (1990) 293.
3 M. Nicolini (ed.), *Platinum and Other Metal Coordination Compounds in Cancer Chemotherapy,* Nijhoff, Boston, MA, 1987.
4 J. Reedijk and J.L. Van Der Veer, *Inorg. Chem., 26* (1987) 1536–1540.
5 T.V. O'Halloran and S.J. Lippard, *Inorg. Chem., 28* (1989) 1289–1295.
6 M.J. Clarke, *Inorg. Chem., 16* (1977) 738–744.
7 M.J. Clarke, *J. Am. Chem. Soc., 100* (1978) 5068–5075.
8 R.E. Shepherd, S. Zhang, F.-T. Lin and R.A. Kortes, *Inorg. Chem., 31* (1992) 1457.
9 S. Zhang, L.A. Holl and R.E. Shepherd, *Inorg. Chem., 29* (1990) 1012–1022.
10 W.D. Harman and H. Taube, *J. Am. Chem. Soc., 110* (1988) 2439.
11 D.W. Harman, J.F. Wishart and H. Taube, *Inorg. Chem., 28* (1989) 2411.
12 S. Zhang and R.E. Shepherd, *Inorg. Chim. Acta, 163* (1989) 237.
13 W.D. Harman and H. Taube, *J. Am. Chem. Soc., 110* (1988) 5403.
14 J.D. Buhr and H. Taube, *Inorg. Chem., 18* (1979) 2208.
15 P.A. Lay and H. Taube, *Inorg. Chem., 28* (1989) 3561–3564.
16 P.A. Lay, R.H. Magnuson and H. Taube, *Inorg. Chem., 18* (1989) 3001.
17 P.A. Lay, R.H. Magnuson, J. Sen and H. Taube, *J. Am. Chem. Soc., 104* (1982) 7658–7659.
18 C.J. Gilmore, *J. Appl. Crystallogr., 17* (1984) 42–46.
19 DIRDIF, *Tech. Rep. 1984/1,* Crystallographic Laboratory, Toernooivedl, Nijmegen, Netherlands, 1984.
20 M.R. Churchill, *Inorg. Chem., 12* (1973) 1213.
21 D.T. Cromer and J.T. Weber, *International Tables for X-ray Crystallography,* Vol. IV, Kynoch, Birmingham, UK, 1974, Tables 2.2 A and 2.3.1.
22 J.A. Ibers and W.C. Hamilton, *Acta Crystallogr., 17* (1964) 781–782.
23 W.D. Harman, D.P. Fairlie and H. Taube, *J. Am. Chem. Soc., 108* (1986) 8223 –8227.
24 V.M. Rodriguez-Bailey and M.J. Clarke, *Ph.D. Thesis,* Boston College, MA, USA, 1992.
25 M.J. Clarke and H. Taube, *J. Am. Chem. Soc., 96* (1974) 5413–5419.
26 M.J. Clarke and H. Taube, *J. Am. Chem. Soc., 97* (1975) 1397–1403.
27 K. Krogh-Jespersen, J.D. Westbrook, J.A. Potenza and H.J. Schugar, *J. Am. Chem. Soc., 109* (1987) 7025–7031.
28 P.A. Lay, R.H. Magnuson and H. Taube, *Inorg. Chem., 27* (1988) 2848–2853.
29 M.E. Kastner, K.F. Coffey, M.J. Clarke, S.E. Edmonds and K. Eriks, *J. Am. Chem. Soc., 103* (1981) 5747–5752.
30 M. Ghosh, A.K. Basak, S.K. Mazumdar and B. Sheldrick, *Acta Crystallogr., Sect. C, 47* (1991) 577–580.
31 H. Krentzien, M.J. Clarke and H. Taube, *Bioinorg. Chem., 4* (1975) 143–151.
32 J. Gulens and J. Page, *Electroanal. Chem. Interfacial Electrochem., 55* (1974) 239–253.
33 W.D. Harman and H. Taube, *J. Am. Chem. Soc., 112* (1990) 2261–2263.